GEOPHYSICS, VOL. 63, NO. 3 (MAY-JUNE 1998); P. 957–969, 9 FIGS., 1 TABLE.

Feasibility of nonhyperbolic moveout inversion in transversely isotropic media

Vladimir Grechka* and Ilya Tsvankin*

ABSTRACT

Inversion of reflection traveltimes in anisotropic media can provide estimates of anisotropic coefficients required for seismic processing and lithology discrimination. Nonhyperbolic P-wave moveout for transverse isotropy with a vertical symmetry axis (VTI media) is controlled by the parameter η (or, alternatively, by the horizontal velocity V_{hor}), which is also responsible for the influence of anisotropy on all time-processing steps, including dip-moveout (DMO) correction and time migration. Here, we recast the nonhyperbolic moveout equation, originally developed by Tsvankin and Thomsen, as a function of V_{hor} and normal-moveout (NMO) velocity V_{nmo} and introduce a correction factor in the denominator that increases the accuracy at intermediate offsets. Then we apply this equation to obtain V_{hor} and η from nonhyperbolic semblance analysis on long common midpoint (CMP) spreads and study the accuracy and stability of the inversion procedure.

Our error analysis shows that the horizontal velocity becomes relatively well-constrained by reflection traveltimes if the spreadlength exceeds twice the reflector depth. There is, however, a certain degree of tradeoff between V_{hor} and V_{nmo} caused by the interplay between the quadratic and quartic term of the moveout series. Since the errors in V_{hor} and V_{nmo} have opposite signs, the *absolute* error in the parameter η (which depends on the ratio V_{hor}/V_{nmo}) turns out to be at least two times bigger than the percentage error in V_{hor}. Therefore, the inverted value of η is highly sensitive to small correlated errors in reflection traveltimes, with moveout distortions on the order of 3–4 ms leading to errors in η up to ± 0.1—even in the simplest model of a single VTI layer. Similar conclusions apply to vertically inhomogeneous media, in which the interval horizontal velocity can be obtained with an accuracy often comparable to that of the NMO velocity, while the interval values of η are distorted by the tradeoff between V_{hor} and V_{nmo} that gets amplified by the Dix-type differentiation procedure.

We applied nonhyperbolic semblance analysis to a walkaway VSP data set acquired at Vacuum field, New Mexico, and obtained a significant value of $\eta = 0.19$ indicative of nonnegligible anisotropy in this area. Then we combined moveout inversion results with the known vertical velocity to resolve the anisotropic coefficients ϵ and δ. However, in agreement with our modeling results, η estimation was significantly compounded by the scatter in the measured traveltimes.

Certain instability in η inversion has no influence on the results of anisotropic poststack time migration because all kinematically equivalent models obtained from nonhyperbolic moveout give an adequate description of long-spread reflection traveltimes. Also, inversion of nonhyperbolic moveout provides a relatively accurate horizontal-velocity function that can be combined with the vertical velocity (if it is available) to estimate the anisotropic coefficient ϵ. However, η represents a valuable lithology indicator that can be obtained from surface P-wave data. Therefore, for purposes of lithology discrimination, it is preferable to find η by means of the more stable DMO method of Alkhalifah and Tsvankin.

INTRODUCTION

Conventional hyperbolic moveout analysis, routinely used for building isotropic velocity models, is insufficient for velocity estimation in anisotropic media. If the medium is transversely isotropic with a vertical symmetry axis (VTI), the NMO velocities from horizontal reflectors of all three pure modes (P, SV, and SH)[1] differ from the corresponding vertical velocities

[1]For brevity, the qualifiers in "quasi-P-wave" and "quasi-SV-wave" are omitted.

Manuscript received by the editor August 15, 1996; revised manuscript received September 22, 1997.
*Colorado School of Mines, Department of Geophysics, Center for Wave Phenomena, 13th & Maple Streets, Golden, CO 80401. E-mail addresses: vgrechka@dix.mines.edu; ilya@dix.mines.edu.

(Thomsen, 1986):

$$V_{\rm nmo}\,[P\text{-wave}] = V_{P0}\sqrt{1+2\delta}, \tag{1}$$

$$V_{\rm nmo}\,[SV\text{-wave}] = V_{S0}\sqrt{1+2\sigma}, \tag{2}$$

and

$$V_{\rm nmo}\,[SH\text{-wave}] = V_{S0}\sqrt{1+2\gamma}, \tag{3}$$

where V_{P0} and V_{S0} are the vertical P- and S-wave velocities, respectively, and ϵ, δ, and γ are Thomsen's (1986) anisotropy parameters. The coefficient $\sigma \equiv (V_{P0}/V_{S0})^2(\epsilon-\delta)$ is largely responsible for SV-wave kinematic signatures in VTI media (Tsvankin and Thomsen, 1994). A detailed discussion of notation for transversely isotropic media can be found in Tsvankin (1996).

From equations (1)–(3) it is clear that NMO velocities and conventional-spread reflection moveout as a whole do not provide enough information to recover the anisotropic coefficients, even if both P and shear data have been recorded. This explains the importance of using nonhyperbolic (long-spread) reflection moveout in the reconstruction of the anisotropic velocity field. In the presence of transverse isotropy, moveout becomes nonhyperbolic even in a single homogeneous VTI layer unless the anisotropy is elliptical. Tsvankin and Thomsen (1994) have developed a nonhyperbolic moveout equation that reduces to the exact quartic Taylor series for the t^2-x^2 curve at small source-receiver offsets and converges at infinitely large offsets as well. This equation provides a good fit to P-wave long-spread reflection moveout in horizontally stratified VTI media with no restrictions on the magnitude of the velocity variations.

Originally, Tsvankin and Thomsen (1994) formulated their moveout equation in terms of the generic Thomsen parameters V_{P0}, V_{S0}, ϵ, and δ. Alkhalifah and Tsvankin (1995), however, showed that P-wave reflection moveout is largely controlled by just two parameter combinations—the NMO velocity from a horizontal reflector ($V_{\rm nmo}$) responsible for short-spread moveout [equation (1)] and the anisotropic coefficient η, which determines the nonhyperbolic portion of the moveout curve:

$$\eta \equiv \frac{1}{2}\left(\frac{V_{\rm hor}^2}{V_{\rm nmo}^2}-1\right) = \frac{\epsilon-\delta}{1+2\delta}, \tag{4}$$

where

$$V_{\rm hor} = V_{\rm nmo}\sqrt{1+2\eta} \tag{5}$$

is the horizontal velocity. Therefore, P-wave moveout data are not sufficient to resolve the true vertical velocity, no matter how large the maximum offset. Tsvankin and Thomsen (1995) demonstrated that the only way to obtain the vertical velocity and anisotropic coefficients from reflection traveltimes is to include long-spread moveout of the SV-wave in the inversion procedure.

The work of Alkhalifah and Tsvankin (1995), however, proves that it is not necessary to know the individual values of the anisotropic parameters and the vertical velocity for P-wave *time* processing. All time-processing steps, including NMO, DMO, and time migration, are fully determined by the two parameters ($V_{\rm nmo}$ and η) responsible for reflection moveout. Alkhalifah and Tsvankin developed an inversion procedure designed to obtain $V_{\rm nmo}$ and η from moveout velocities measured for two different reflector dips. In the most common case, $V_{\rm nmo}$ can be found directly by conventional semblance analysis of horizontal events, which allows one to determine η from the NMO velocity of an additional dipping event. Although this methodology provides a relatively stable way of estimating the parameter η, it requires the presence of dipping reflectors (such as fault planes) under the formation of interest.

Long-spread P-wave moveout from horizontal reflectors represents an alternative source of information about η. Alkhalifah (1997) suggested estimating $V_{\rm nmo}$ and η (or $V_{\rm nmo}$ and $V_{\rm hor}$) by a 2-D semblance scan based on the nonhyperbolic moveout equation described earlier. He showed that this inversion procedure gives reasonably accurate results for data acquired over a horizontally homogeneous VTI layer. However, he also found that the extracted values of η are sensitive to small errors in $V_{\rm nmo}$, even if the spreadlength is twice as large as the reflector depth. This tradeoff stems from the ambiguity in the determination of the quartic P-wave moveout term first described by Tsvankin and Thomsen (1995). Tsvankin and Thomsen did not use, however, a two-parameter representation of P-wave reflection moveout (introduced later by Alkhalifah and Tsvankin, 1995) and were dealing with a more complicated problem of recovering three moveout coefficients at each value of the vertical time.

Here, we introduce a correction into the nonhyperbolic moveout equation of Tsvankin and Thomsen (1994) that makes it even more accurate at intermediate offsets most important for nonhyperbolic moveout analysis. The modified equation is used to investigate the stability of the inversion of long-spread P-wave moveout data acquired in the presence of random and correlated noise. We start with the simplest model of a single VTI layer and then extend our results to vertically inhomogeneous media using a Dix-type differentiation procedure that involves the nonhyperbolic term of the moveout equation. The error analysis shows that the horizontal velocity is relatively well constrained by long-spread moveout, provided the spreadlength exceeds two reflector depths, with errors that are not much higher than those in the NMO velocity. In contrast, the parameter η is influenced by the tradeoff between the horizontal and NMO velocity and, therefore, is more sensitive to correlated errors in the reflection traveltimes.

ANALYSIS OF LONG-SPREAD *P*-WAVE MOVEOUT

Our description of P-wave reflection traveltimes on long-spread CMP gathers is based on the nonhyperbolic moveout equation developed by Tsvankin and Thomsen (1994) and rewritten in terms of the parameter η by Alkhalifah and Tsvankin (1995). In a single horizontal VTI layer, this moveout approximation has the form

$$t^2(x) = t_0^2 + \frac{x^2}{V_{\rm nmo}^2} - \frac{2\eta x^4}{V_{\rm nmo}^2\left[t_0^2\,V_{\rm nmo}^2 + (1+2\eta)\,x^2\right]}, \tag{6}$$

where t_0 is the two-way vertical traveltime and x is the source-receiver offset; $V_{\rm nmo}$ and η are defined in equations (1) and (4). The only difference between equation (6) and the original expression of Tsvankin and Thomsen (1994) is that the contribution of the S-wave vertical velocity V_{S0} to P-wave moveout is ignored.

Introducing the horizontal velocity [equation (5)], we rewrite equation (6) as

$$t^2(x) = t_0^2 + \frac{x^2}{V_{\rm nmo}^2} - \frac{\left(V_{\rm hor}^2 - V_{\rm nmo}^2\right) x^4}{V_{\rm nmo}^2 \left(t_0^2\, V_{\rm nmo}^4 + V_{\rm hor}^2\, x^2\right)}. \qquad (7)$$

To obtain a quantitative picture of the influence of $V_{\rm nmo}$ and $V_{\rm hor}$ (or η) on long-spread moveout, we perform a numerical analysis of the nonhyperbolic moveout equation (7). Figure 1 shows the dependence of reflection moveout on variations in $V_{\rm nmo}$ and $V_{\rm hor}$ for a model with a moderate positive value of $\eta = 0.16$ that was observed on field data (Alkhalifah et al., 1996). Note two interesting features of the maximum traveltime differences $\Delta t_{\rm max}$ displayed in Figure 1. First, the contours of $\Delta t_{\rm max}$ form an elongated "valley" in the coordinates ($V_{\rm nmo}$, $V_{\rm hor}$), along which the traveltimes remain almost independent of the moveout parameters. The changes in $V_{\rm nmo}$ and $V_{\rm hor}$ within this valley of similar moveout curves are comparable but have opposite signs. Since η is determined by the ratio $V_{\rm hor}/V_{\rm nmo}$ [equation (4)], the variation in η over the range of these kinematically equivalent models is close to the sum of the corresponding percentage changes in the horizontal and NMO velocity. As a result, a certain relative error in $V_{\rm hor}$ can be expected to translate into at least twice as large absolute error in the parameter η.

Second, the center of the contours is somewhat shifted from the correct position ($V_{\rm nmo} = 2.0$ km/s, $V_{\rm hor} = 2.3$ km/s) due to small deviations of the moveout approximation (7) from the ray-traced traveltime curve for the reference model. Also, for the same reason the minimum value of $\Delta t_{\rm max}$ is not equal to zero. The best-fit η that corresponds to the model with the smallest time residual is equal to 0.13 instead of the actual 0.16. The error increases in VTI media with more pronounced

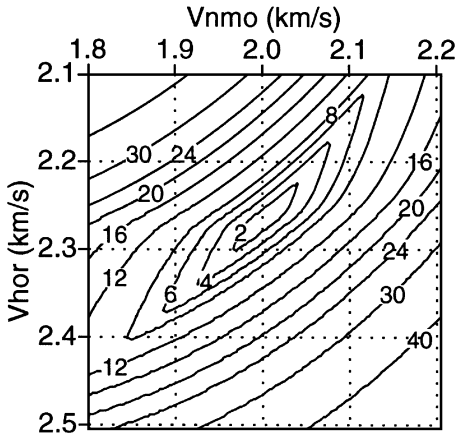

FIG. 1. The influence of $V_{\rm nmo}$ and $V_{\rm hor}$ on the P-wave reflection traveltimes in a horizontal VTI layer. The contours display the maximum difference $\Delta t_{\rm max}$ (in milliseconds) between the traveltimes for a reference model and models with the same t_0 but different $V_{\rm nmo}$ and $V_{\rm hor}$ shown on the axes; the spreadlength $x_{\rm max} = 2$ km ($x_{\rm max}/h = 2$). The model parameters are $t_0 = 1.0$ s, $V_{\rm nmo} = 2.0$ km/s, and $V_{\rm hor} = 2.3$ km/s; the corresponding $\eta = 0.16$ (Thomsen's parameters of the model are $V_{P0} = 2.0$ km/s, $\epsilon = 0.16$, and $\delta = 0$; the reflector depth $h = 1$ km). The moveout for the reference model is calculated using ray tracing, while the traveltimes for all other models are computed from equation (7).

nonhyperbolic moveout (larger η), and for a model with $\eta = 0.3$ the best-fit value is as low as $\eta = 0.24$. Thus, algorithms based on equations (6) or (7), such as the one of Alkhalifah (1997), always underestimate the value of η. This translation of small deviations of equation (7) from the exact traveltimes into sizable errors in η is an indication of relatively low sensitivity of reflection moveout to this parameter (i.e., η may change significantly within the family of equivalent models described above).

Equation (7) was designed to ensure the correct behavior of the moveout for infinitely large offsets ($x \to \infty$). At intermediate offsets ($x/h \approx 2$, h is the reflector depth), however, this moveout approximation can be somewhat improved by empirically changing the denominator of the nonhyperbolic term. We found that introducing the coefficient $C = 1.2$ in front of $V_{\rm hor}^2\, x^2$ minimizes deviations from the exact traveltimes for the most practical range of offsets $1.5h < x < 2.5h$. This modification changes the moveout at large offsets yet keeps the correct values of the quadratic and quartic moveout coefficients. Thus, hereafter for the single-layer model we will use the following version of equation (7):

$$t^2(x) = t_0^2 + \frac{x^2}{V_{\rm nmo}^2} - \frac{\left(V_{\rm hor}^2 - V_{\rm nmo}^2\right) x^4}{V_{\rm nmo}^2 \left(t_0^2\, V_{\rm nmo}^4 + C\, V_{\rm hor}^2\, x^2\right)}, \qquad (8)$$

with $C = 1.2$. Figure 2 shows contours similar to the ones in Figure 1 but now calculated using the modified approximation (8) for three different spreadlength-to-depth ratios. The correction in the traveltime equation has moved the center of the contours $\Delta t_{\rm max}$ in Figure 2 to the correct position, corresponding to $V_{\rm nmo} = 2.0$ km/s and $V_{\rm hor} = 2.3$ km/s, as well as substantially reduced the traveltime residuals ($\Delta t_{\rm max}$) at the center of the contours.

As expected, Figure 2 indicates that both $V_{\rm hor}$ and the corresponding η become better constrained with increasing maximum offset $x_{\rm max}$. With growing $x_{\rm max}/h$, the contours for a given maximum time residual become tighter and tilt toward the $V_{\rm nmo}$-axis, thus making the variation in $V_{\rm hor}$ for a fixed $\Delta t_{\rm max}$ less pronounced. The meaning of this result becomes clear if we recall that $V_{\rm hor}$ and η are responsible for the nonhyperbolic moveout term, which makes a significant contribution to the traveltime only at offsets exceeding the reflector depth. Therefore, the inversion of nonhyperbolic moveout for $V_{\rm hor}$ and η becomes more stable with increasing spreadlength. However, it is seldom possible to use spreads $x_{\rm max} > 2.5h$ in practice because of the limitations of the conventional acquisition design.

In addition to analyzing the maximum traveltime differences, it is instructive to examine reflection moveout on the whole CMP spread. Figure 3 shows ray-traced traveltime curves for the models labeled A, B, and C in Figure 2b. Despite a significant variation in η (from 0.09 to 0.24) among the three models, the maximum values of the traveltime differences (Δt_{AB} and Δt_{CB}) picked from Figure 2b are about 3 ms. Figure 3, generated using an exact ray-tracing algorithm, confirms this result: the moveouts t_A, t_B, and t_C are very close to each other at all offsets, with the maximum deviations smaller than 3 ms. Again, the absolute variation in η from model A to model C is somewhat larger than the sum of the corresponding relative changes in $V_{\rm nmo}$ and $V_{\rm hor}$ (which are close to ± 2.5–3%). Note that the maximum separation between the curves occurs

at an intermediate offset equal to the reflector depth h rather than at the largest offset $x_{max} = 2h$.

The conclusions drawn from Figures 2 and 3 have important consequences for evaluating the feasibility of nonhyperbolic moveout inversion. For spreadlength reaching twice the reflector depth, the horizontal velocity becomes almost as tightly constrained by reflection traveltimes as the NMO velocity. At the same time, the absolute variation in η over the family of kinematically equivalent models is at least twice as large as the corresponding relative change in V_{hor}. Hence, we can expect that even small long-period traveltime errors may result in significant deviations of η from the correct value. Below, we verify this conclusion by performing the actual inversion of long-spread moveout in the presence of different kinds of traveltime errors.

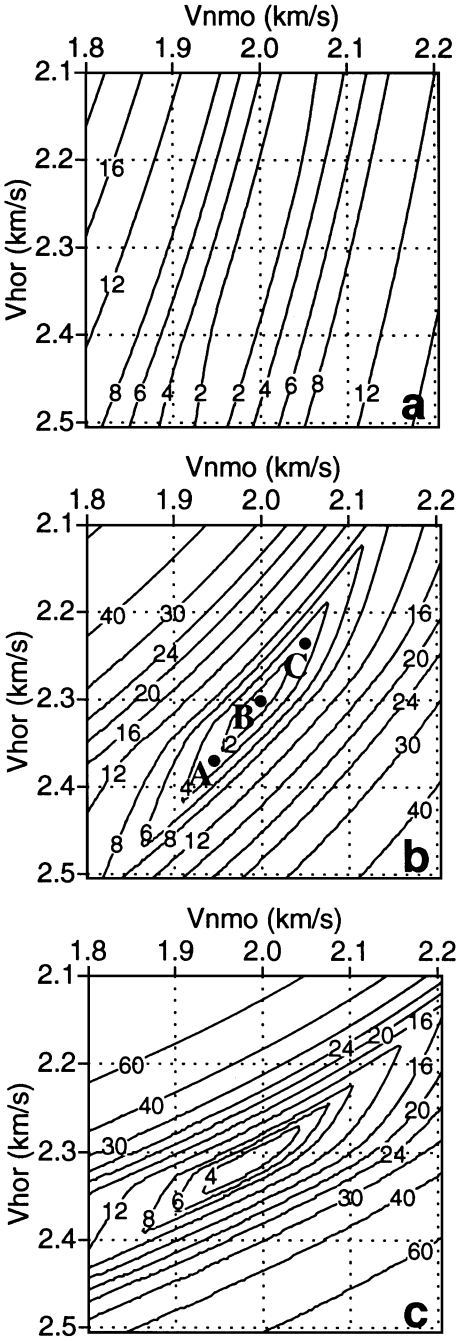

FIG. 2. The same contours as in Figure 1 but calculated using equation (8). The model parameters are $V_{nmo} = 2$ km/s and $V_{hor} = 2.3$ km/s ($\eta = 0.16$). The plots correspond to three different spreadlengths: $x_{max}/h = 1$ (a); $x_{max}/h = 2$ (b); and $x_{max}/h = 3$ (c).

INVERSION OF NONHYPERBOLIC MOVEOUT

Nonhyperbolic semblance search

If reflection traveltimes on a certain spreadlength are known, the parameters t_0, V_{nmo}, and V_{hor} can be obtained, for instance, by least-squares fitting of equation (8) to the moveout curve (see the real-data example following). However, due to the presence of noise and the need to automate data processing, picking of reflection traveltimes on CMP data is seldom done in practice. Instead, the best-fit moveout (stacking) velocity and the corresponding hyperbolic moveout curve are usually found from semblance analysis on CMP gathers, preferably with

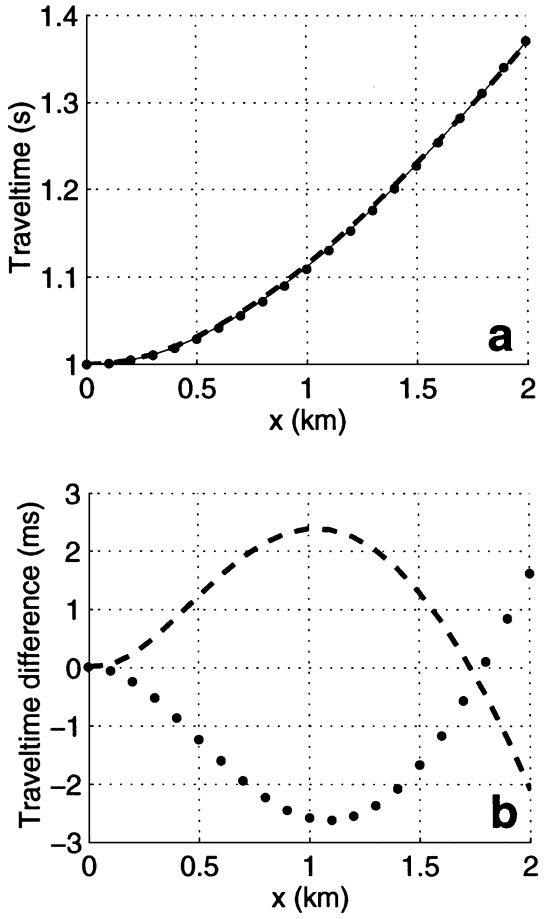

FIG. 3. (a) Reflection moveouts (t_A, t_B, and t_C) obtained by ray tracing for the models marked by A (dashed), B (thin solid), and C (dotted) in Figure 2b. (b) The traveltime differences $\Delta t_{AB} = t_A - t_B$ (dashed) and $\Delta t_{CB} = t_C - t_B$ (dotted). The parameters are $V_{nmo} = 1.95$ km/s, $V_{hor} = 2.37$ km/s, $\eta = 0.24$ (model A); $V_{nmo} = 2.0$ km/s, $V_{hor} = 2.3$ km/s, $\eta = 0.16$ (model B); and $V_{nmo} = 2.05$ km/s, $V_{hor} = 2.23$ km/s, $\eta = 0.09$ (model C).

spreadlength close to reflector depth (Taner and Koehler, 1969; Neidell and Taner, 1971). Similarly, the inversion for V_{hor} or η can be accomplished by semblance analysis along nonhyperbolic moveout curves (Alkhalifah, 1996). For a given value of the vertical traveltime t_0, one now needs to carry out a 2-D semblance scan over V_{nmo} and V_{hor} to find a model that yields the maximum value of semblance. The semblance coefficient was calculated as (Taner and Koehler, 1969)

$$S(t_0, V_{nmo}, \eta) = \frac{\sum_{t_0'=t_0-T/2}^{t_0+T/2} \left[\sum_{x=x_{min}}^{x_{max}} F(x,t) \right]^2}{M \sum_{t_0'=t_0-T/2}^{t_0+T/2} \sum_{x=x_{min}}^{x_{max}} F^2(x,t)}, \qquad (9)$$

where M is the number of traces. The summation of the amplitudes $F(x,t)$ and their squares $F^2(x,t)$ in equation (9) is performed along the nonhyperbolic moveout curves $t(t_0', V_{nmo}, V_{hor}, x)$ [described by equation (8)] originated at the vertical traveltimes t_0' within a smoothing window T centered at time t_0.

In the following examples, we generated reflected arrivals by combining ray-traced traveltimes with a wavelet that has the same shape and amplitude at all offsets. The traces were equally spaced with a 40-m interval; for the most typical maximum offset $x_{max} = 2h = 2.0$ km used below, that gives $M = 50$. The smoothing window was $T = 20$ ms long, which corresponds to five time samples. The amplitudes $F(x,t)$ between time samples were obtained by linear interpolation.

Analysis of numerical results

The results of the nonhyperbolic semblance search for a single-layer VTI model are displayed in Figure 4. The coordinates of the semblance maximum are close to the actual parameters V_{nmo} and V_{hor}; therefore, we obtain a sufficiently accurate estimate of η as well. [Note that application of the original equation (7) leads to errors in all three parameters, particularly in η.] The shape of the semblance contours in Figures 4b and 4c and the contours of the maximum traveltime difference in Figure 2b look quite similar. This can be expected because the semblance values for models with close traveltime curves cannot differ much from each other. Again, V_{nmo} and V_{hor} can vary simultaneously along the diagonal "ridge" in the semblance contours without producing significant changes in the values of semblance (Figure 4). Confirming our conclusion based on traveltime analysis, Figure 4 shows that within this family of models with close semblances, higher values of V_{nmo} are compensated by lower values of V_{hor} and absolute variations in η are at least twice as large as the corresponding percentage changes in V_{hor}.

The influence of spreadlength on the sensitivity of reflection moveout (this time measured by the value of semblance) to V_{nmo} and V_{hor} is illustrated by Figure 5. For the relatively short (in the context of nonhyperbolic moveout inversion) spreadlength of $1.5h$ in Figure 5a, the contours are tilted toward the V_{hor}-axis and the horizontal velocity is constrained much less tightly than is V_{nmo}. However, for a longer (but still feasible) spread equal to twice the reflector depth (Figure 5b), the range of variation in V_{hor} within the family of kinematically equivalent models becomes closer to that of V_{nmo}. For less common spreadlengths close to or exceeding $2.5h$ (Figures 5c and 5d), the horizontal velocity has even more influence on the semblance values than does the NMO velocity. Asymptotically, for infinitely large offsets the effective moveout velocity approaches V_{hor} and the reflection moveout is controlled by the horizontal velocity.

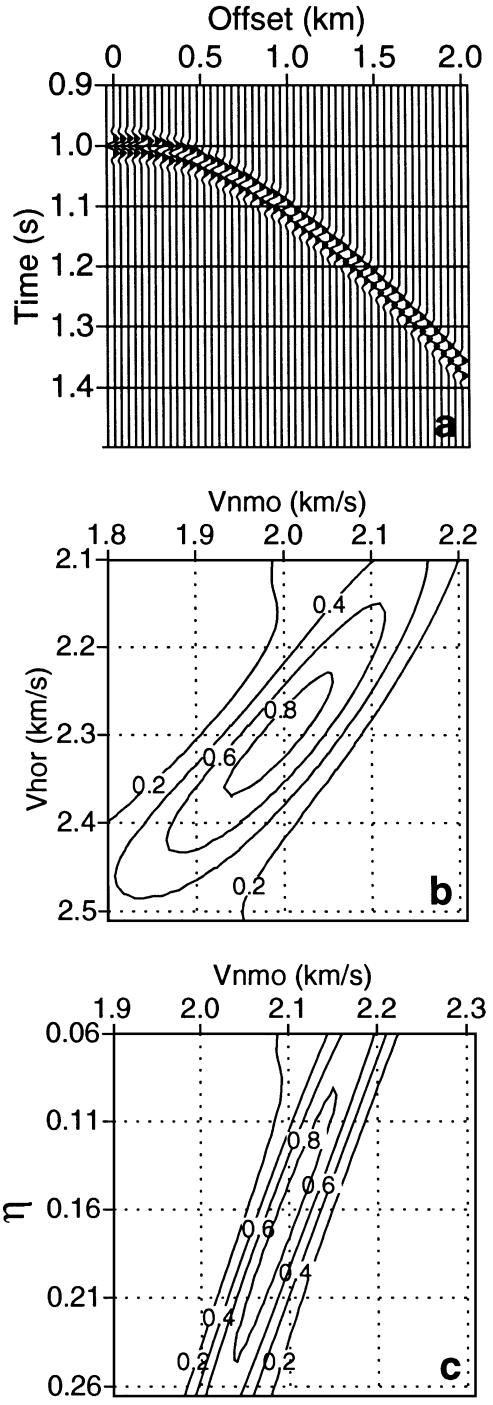

FIG. 4. (a) Synthetic seismogram of the P-wave reflected from the bottom of a VTI layer with the same parameters as in Figures 1 and 2: $t_0 = 1$ s, $V_{nmo} = 2$ km/s, and $V_{hor} = 2.3$ km/s ($\eta = 0.16$). The spreadlength is equal to two reflector depths; the source pulse is a Ricker wavelet with the central frequency 40 Hz. (b) Semblance contours in the coordinates V_{nmo} and V_{hor} calculated using equation (8) for $t_0 = 1$ s. (c) Same as (b), but expressed through V_{nmo} and η.

Influence of traveltime errors on V_{hor} and η

Here, we continue with a more detailed analysis of the stability of the inversion procedure. To study the influence of realistic traveltime distortions, we added an error function $\tau(x)$ to the reflection traveltimes $t(x)$ from Figure 4 (without changing the trace amplitudes) and performed 2-D semblance analysis of the modified seismograms. Although the magnitude of the traveltime error was small (several ms), it could be expected to cause substantial errors in η (Figure 4).

The function $\tau(x)$ in Figure 6a was chosen to coincide with the time resudual for model A (Figures 2b and 3b). The maximum of $\tau(x)$ in this case is less than one time sample (4 ms) in conventional processing, and its predominant period is between $1.5x_{max}$ and $2x_{max}$, where x_{max} is the spreadlength. Such a class of time distortions may result from contamination of reflection times by coherent noise (errors in the statics correction, ambient noise, etc.) or by the influence of small high- or low-velocity lenses.

In accordance with the form of the error function, the pair ($V_{nmo} = 1.96$ km/s, $V_{hor} = 2.36$ km/s) that provides the maximum semblance in Figure 6a practically coincides with the parameters of model A [a small difference is due to the slight inaccuracy of equation (8)]. Note that the semblance maximum moves along the diagonal ridge in Figure 4b, with the increase in V_{hor} compensated by the smaller value of V_{nmo}. While V_{nmo} and V_{hor} are off by only -2% and $+2.6\%$, respectively, the opposite sign of these errors yields the best-fit value of $\eta = 0.23$ instead of the correct $\eta = 0.16$.

Figure 6b shows the result of the semblance analysis with the error function equal to the time residual for model C from Figures 2b and 3b. As expected, the coordinates of the semblance maximum in this case are close to the parameters of model C ($V_{nmo} = 2.05$ km/s, $V_{hor} = 2.25$ km/s, $\eta = 0.1$), with the error in η equal to (-0.06). Thus, a low-frequency noise function with a magnitude of up to ± 3 ms leads to the variation in η between 0.1 and 0.23.

In Figure 6c, we reproduced Figure 6a with the addition of random noise on top of the traveltime residual for model A. The values of semblance became substantially smaller, and the semblance maximum moved a little bit further from the actual solution. The best-fit η in this case is equal to 0.25, which is 0.09 higher than the actual value. In general, the shape of the semblance objective function is not sensitive to purely random errors in the traveltimes.

Similar results were obtained for other slowly varying error functions with a small magnitude. For instance, Figure 6d was generated for a linear error function equal to 4 ms at zero offset and $(-4$ ms) at the end of spread. Such an error mitigates the increase in traveltime with offset, and the effective NMO velocity becomes higher. To provide a good fit at large offsets, the horizontal velocity must be smaller than the actual value, and the semblance analysis yields $V_{nmo} = 2.07$ km/s and $V_{hor} = 2.24$ km/s. The corresponding η is as low as 0.085, which is about one-half of the actual value.

The results of semblance analysis in Figure 6 confirm the conclusion drawn from the study of reflection traveltimes (Figures 2 and 3): the horizontal velocity is almost as tightly

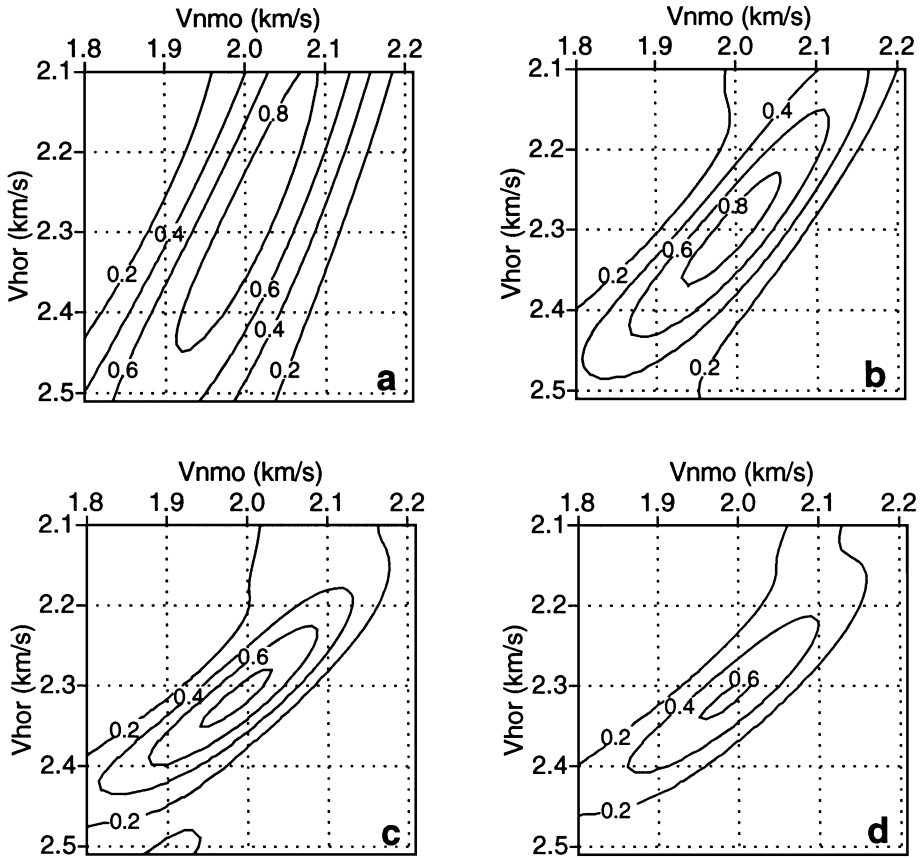

FIG. 5. Semblance contours at different spreadlengths plotted in coordinates (V_{nmo}, V_{hor}). (a) $x_{max}/h = 1.5$; (b) $x_{max}/h = 2$; (c) $x_{max}/h = 2.5$; (d) $x_{max}/h = 3$. The model parameters are the same as those in Figure 4.

controlled by reflection moveout as $V_{\rm nmo}$, provided the spread-length is no smaller than two reflector depths. In contrast, long-period traveltime errors that can be considered as insignificant in the practice of data processing may cause errors in inverted value of η reaching ± 0.1. These errors are entirely due to the tradeoff between $V_{\rm nmo}$ and $V_{\rm hor}$ on long-spread gathers (i.e., if we knew the correct value of $V_{\rm nmo}$, we could determine $V_{\rm hor}$ and η with high accuracy).

NONHYPERBOLIC VELOCITY ANALYSIS FOR LAYERED MEDIA

The discussion above was limited to moveout inversion in the simplest single-layer model. Tsvankin and Thomsen (1994) have shown that their nonhyperbolic equation remains valid in horizontally layered media as well, provided the moveout coefficients are replaced by effective values that include the influence of the vertical inhomogeneity above the reflector. They also have developed a Dix-type differentiation procedure to estimate the interval values of the quartic moveout coefficient. Here, we apply their expressions in a somewhat modified form by introducing the interval and effective values of the parameter η and ignoring the contribution of the shear-wave vertical velocity V_{S0} [see Appendix A and Alkhalifah (1997)].

Following Appendix A, P-wave traveltimes for reflections from the ith ($i = 1, \ldots, N$) interface in vertically stratified VTI media can be described by an expression that has the same form as the single-layer equation (8):

$$t^2(x) = t_0^2(i) + \frac{x^2}{V_{\rm nmo}^2(i)} - \frac{\left[V_{\rm hor}^2(i) - V_{\rm nmo}^2(i)\right] x^4}{V_{\rm nmo}^2(i)\left[t_0^2(i)\, V_{\rm nmo}^4(i) + C\, V_{\rm hor}^2(i)\, x^2\right]}. \quad (10)$$

The value of the coefficient C is discussed below.

The NMO velocity $V_{\rm nmo}(i)$ is computed through the interval values using the conventional Dix (1955) equation,

$$V_{\rm nmo}^2(i) = \frac{1}{t_0(i)} \sum_{i=1}^{N} V_{{\rm nmo},i}^2\, t_{0,i}, \quad (11)$$

while the effective horizontal velocity for layered media is defined as

$$V_{\rm hor}(i) = V_{\rm nmo}(i)\sqrt{1 + 2\eta(i)}, \quad (12)$$

with the effective $\eta(i)$ given by

$$\eta(i) = \frac{1}{8}\left\{\frac{1}{V_{\rm nmo}^4(i)\, t_0(i)} \times \left[\sum_{i=1}^{N} V_{{\rm nmo},i}^2\left[4V_{{\rm hor},i}^2 - 3V_{{\rm nmo},i}^2\right] t_{0,i}\right] - 1\right\}. \quad (13)$$

$V_{{\rm nmo},i}$, $V_{{\rm hor},i}$, and $t_{0,i}$ are the interval values in layer i.

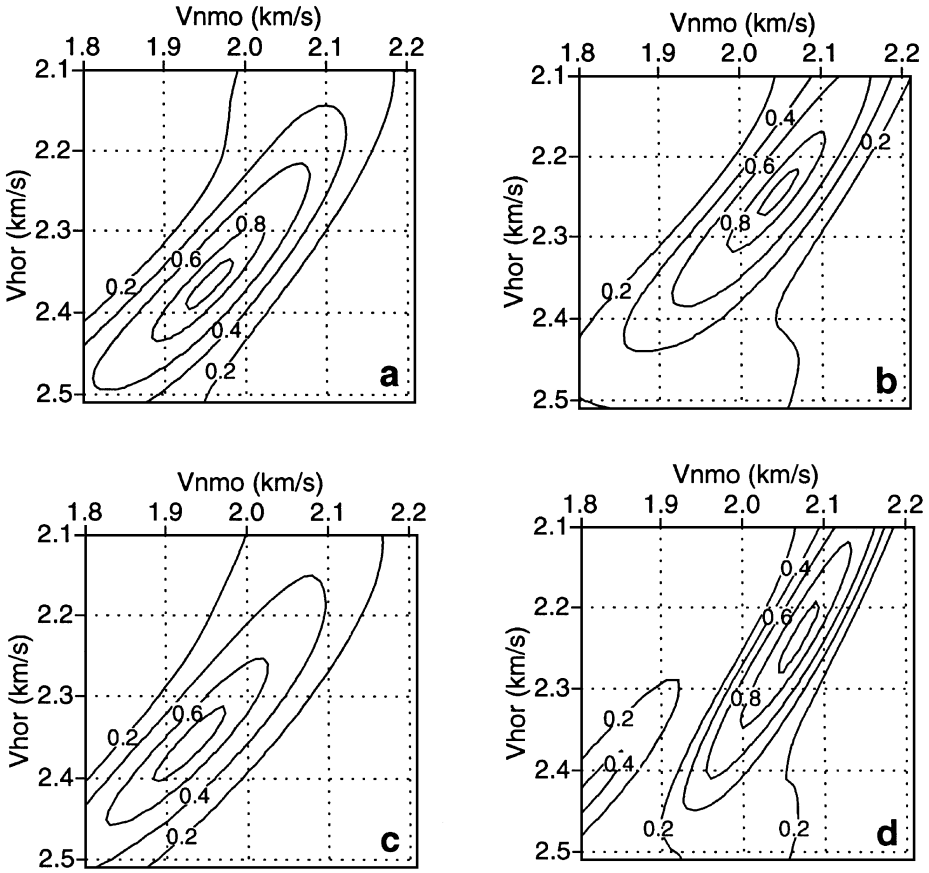

FIG. 6. Results of semblance analysis for the model from Figure 4 after the addition of traveltime errors with small magnitude. (a) The traveltime error is equal to the residual for model A from Figure 2b (see Figure 3b); (b) the error is equal to the residual for model C from Figure 2b (see Figure 3b); (c) same as (a) plus random noise with a magnitude of 3 ms; (d) linear error function with $\tau(0) = 4$ ms and $\tau(x_{\rm max}) = -4$ ms.

Equations (10)–(13) provide a basis for a layer-stripping approach that can be summarized as follows (for more details, see Appendix A).

1) Using long-spread P-wave moveout for the ith ($i = 1, \ldots, N$) interface, find $t_0(i)$, $V_{\rm nmo}(i)$, and $V_{\rm hor}(i)$ from semblance analysis along nonhyperbolic moveout curves described by equation (10). [Clearly, for the bottom of shallowest layer ($i = 1$), the effective and interval values are equal to one another.]
2) Compute the interval NMO velocity in any layer $i = 2, \ldots, N$ from the Dix equation

$$V_{{\rm nmo},i}^2 = \frac{V_{\rm nmo}^2(i)\, t_0(i) - V_{\rm nmo}^2(i-1)\, t_0(i-1)}{t_0(i) - t_0(i-1)}. \tag{14}$$

3) Using equations (12) and (13), compute an auxiliary effective parameter

$$f(i) \equiv V_{\rm nmo}^2(i)\left[4V_{\rm hor}^2(i) - 3V_{\rm nmo}^2(i)\right] = \frac{1}{t_0(i)} \sum_{i=1}^{N} V_{{\rm nmo},i}^2 \left[4V_{{\rm hor},i}^2 - 3V_{{\rm nmo},i}^2\right] t_{0,i} \tag{15}$$

for the reflections from the top and bottom of the layer of interest.
4) Carry out the Dix differentiation of $f(i)$ [equation (15)] to obtain the interval values of the horizontal velocity and η:

$$V_{{\rm hor},i} = V_{{\rm nmo},i} \times \sqrt{\frac{1}{4V_{{\rm nmo},i}^4} \frac{f(i)\, t_0(i) - f(i-1)\, t_0(i-1)}{t_0(i) - t_0(i-1)} + \frac{3}{4}} \tag{16}$$

and

$$\eta_i = \frac{1}{8V_{{\rm nmo},i}^4} \times \left[\frac{f(i)\, t_0(i) - f(i-1)\, t_0(i-1)}{t_0(i) - t_0(i-1)} - V_{{\rm nmo},i}^4\right]. \tag{17}$$

First, it is necessary to show that equation (10) [with the effective parameters from equations (11)–(13)] gives an adequate description of P-wave moveout in stratified media. For the single-layer model, we were able to increase the accuracy of our moveout equation on intermediate spreads by choosing $C = 1.2$ in equation (8) [equivalent to equation (10)] instead of $C = 1$ originally used by Alkhalifah and Tsvankin (1995). In the presence of vertical variations in the elastic properties, we do not always find the value $C = 1.2$ to be optimal. Numerical tests performed for various stratified VTI models showed that for a vertical velocity gradient of 0.5-0.6 $\rm s^{-1}$ and relatively small effective η values up to 0.1–0.15 it is preferable to use $C = 1$ or even $C < 1$ (although the accuracy provided by $C = 1.2$ is not much inferior). As was the case for a single layer, the value $C = 1.2$ usually gives an advantage for larger $\eta \geq 0.2$.

It should be mentioned that the traveltimes calculated using $C = 1$ and $C = 1.2$ for the spreadlength-to-depth ratio $x_{\rm max}/h = 2$ are close to each other (in most cases, the difference is less than 0.3–0.5% of t_0). Still, varying C from 1 to 1.2 does have some influence on the inverted value of the effective η because, as shown above, VTI media with substantially different η may have similar traveltimes for spreads $x_{\rm max}/h \approx 2$. In principle, after obtaining a model from nonhyperbolic moveout inversion (using, for instance, $C = 1.2$), it is possible to find the best-fit C by comparison of equation (10) with ray tracing and use this updated value to produce the final inversion result.

Table 1 summarizes the results of a numerical test performed for a model consisting of four homogeneous VTI layers with a typical increase in V_{P0} with depth (the average gradient is close to 0.6 $\rm s^{-1}$) and values of η ranging from zero in the near-surface layer to a maximum of 0.2 in the third layer. The effective moveout coefficients $V_{\rm nmo}(i)$ and $\eta(i)$ obtained from ray-traced seismograms (Figure 7) for all four interfaces using equation (10) are sufficiently close to the analytic values computed from equations (11)–(13). [We did not try to optimize the value of C in equation (10) and used the same $C = 1.2$ as in the single-layer model.] Despite the approximate character of the moveout equation (10) and some amplification of errors during layer stripping, the interval values of $V_{\rm nmo}$ and $V_{\rm hor}$ have been also recovered with acceptable accuracy. Note, however, that the small errors in $V_{\rm nmo}$ and $V_{\rm hor}$ for the two deepest layers have opposite signs (as was the case in the single-layer model), and the errors in interval η in these layers reach 0.06.

Since moveout in stratified media is well described by the same equation that we studied in detail for the homogeneous VTI model, our analysis of the accuracy in the estimation of $V_{\rm nmo}$, $V_{\rm hor}$, and η must remain valid for the effective values of all three parameters. As an example, Figure 8 displays the semblance contours for the reflection from the bottom of the layered model discussed above (Table 1). Again, the contours make up an elongated ridge along which the effective $V_{\rm nmo}(i)$

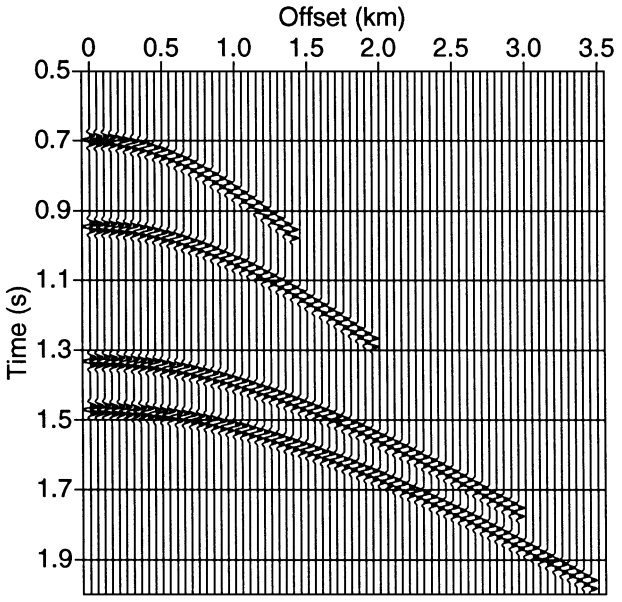

FIG. 7. Synthetic seismograms of P-wave reflections generated by ray tracing for the model from Table 1. The traces were muted to maintain the spreadlength-to-depth ratio of two for all four events.

and $V_{hor}(i)$ can be varied without producing tangible differences in the value of semblance (compare with Figure 4).

The stability of the stripping algorithm is illustrated by the test in Figures 8b and 8c. We introduced errors up to about ±3% in the effective parameters $V_{nmo}(i)$ and $V_{hor}(i)$ for the fourth interface, simulating the movement of the semblance maximum along the ridge in the semblance contours under the influence of long-period traveltime errors with small magnitude (on the order of several milliseconds). As expected, layer stripping magnifies errors in both velocities, but the accuracy of the interval values of V_{nmo} and V_{hor} is comparable. Obviously, errors will increase as the layer gets thinner; still, this and other tests we performed show that layer stripping of the nonhyperbolic moveout term for V_{hor} does not introduce much higher errors than conventional Dix differentiation for the NMO velocity. Therefore, nonhyperbolic moveout inversion can be used to reconstruct the "low-frequency" component of the horizontal velocity as a function of vertical time.

The errors in the interval values of the NMO and horizontal velocity in Figure 8b again have opposite signs. Since interval V_{nmo} and V_{hor} are more distorted than in the single-layer model, the error in interval η easily becomes comparable to η itself (Figure 8c).

FIELD DATA EXAMPLE

We demonstrate the performance of nonhyperbolic moveout inversion and illustrate our error study on a walkaway VSP data set acquired in 1995 by the Reservoir Characterization project of the Colorado School of Mines at Vacuum field in Lea County, New Mexico. The objective of the project was to use both surface seismic and VSP to monitor changes in the properties of a carbonate reservoir caused by CO_2 injection.

We used the data recorded by a downhole receiver placed above the reservoir at a depth of 1005 m. The wavefield was excited at 616 surface source locations with offsets of 60 to 1370 m from the receiver borehole. We picked the traveltimes of the first P-wave arrivals and used them as substitutes for the reflection traveltime from an interface at the receiver depth (Figure 9). The data points plotted in squared coordinates ($t^2 - x^2$) in Figure 9a cluster around a curved line, indicating the presence of substantial nonhyperbolic moveout. Using equation (8), we found a set of moveout parameters that gives the best fit (in the least-squares sense) to the observed traveltimes and plotted the corresponding moveout as a solid line in Figure 9a. Note that the largest offset-to-depth ratio was over 2.7 (the offset should be doubled for comparison with reflection data), which is quite favorable for nonhyperbolic moveout analysis. The inverted values of the NMO and horizontal velocities are $V_{nmo} = 3536$ m/s and $V_{hor} = 4145$ m/s, yielding $\eta = 0.19$.

The rms time residuals for different pairs of V_{nmo} and V_{hor} in Figure 9b look very similar to the contours of the maximum traveltime difference in Figures 1 and 2. The center of the contours corresponds to an rms residual of 6.7 ms; if V_{nmo} and V_{hor} lie on the nearest contour line, the rms residual is equal to 8 ms, a difference of only 1.3 ms. The existence of this family of kinematically equivalent models is in agreement with our modeling results, while the large magnitude of the time residuals is caused by a sizeable scatter in the traveltime measurements. To estimate the error bars on η, we picked the extreme values of η corresponding to the 8-ms contour line (8 ms is close to the minimum rms residual plus one time sample) and obtained $0.09 < \eta < 0.32$.

Since the receiver depth in this case is known, we calculated the average vertical velocity $V_{P0} = 3457$ m/s from the zero-offset traveltime and, using equation (1), found $\delta = 0.02$. Finally, combining the obtained values of η and δ, we determined $\epsilon = 0.22$ (of course, the error bars on ϵ depend on the uncertainty in η). Unfortunately, since only one receiver was deployed, we could not test our layer-stripping algorithm and study the vertical variation in the anisotropic parameters.

Table 1. Accuracy of the nonhyperbolic moveout approximation for *P*-wave reflection traveltimes in layered VTI media. The effective parameters $V_{nmo}(i)$, $V_{hor}(i)$, and $\eta(i)$ ("found") were obtained from semblance velocity analysis [using equation (10) with $C = 1.2$] of synthetic seismograms computed by ray tracing (Figure 7); the spreadlength-to-depth ratio for all events equals 2. The analytic values were calculated from equations (11)–(13). The lower table shows the results of the layer-stripping of the recovered effective parameters [using equations (14)–(17)] versus the actual interval values. The model consists of four homogeneous VTI layers with the following parameters: Layer 1—h (depth of the bottom) = 0.7 km, V_{P_0} = 2.0 km/s, ϵ = 0.05, δ = 0.05; Layer 2—h = 1 km, V_{P_0} = 2.42 km/s, ϵ = 0.15, δ = 0.0417; Layer 3—h = 1.5 km, V_{P_0} = 2.6 km/s, ϵ = 0.3, δ = 0.0714; Layer 4—h = 1.7 km, V_{P_0} = 2.9 km/s, ϵ = 0.2, δ = 0.0469. The corresponding values of V_{nmo}, V_{hor}, and η are given in the table.

Effective values

Layer number	V_{nmo} (km/s) Analytic	Found	Error (%)	V_{hor} (km/s) Analytic	Found	Error (%)	η Analytic	Found	Error (abs)
1	2.098	2.100	0.1	2.098	2.100	0.1	0.000	0.000	0.000
2	2.216	2.225	0.4	2.318	2.340	0.9	0.047	0.053	0.006
3	2.392	2.390	−0.1	2.698	2.760	2.3	0.136	0.167	0.031
4	2.459	2.450	−0.4	2.792	2.860	2.4	0.144	0.181	0.037

Interval values

Layer number	V_{nmo} (km/s) Actual	Found	Error (%)	V_{hor} (km/s) Actual	Found	Error (%)	η Actual	Found	Error (abs)
1	2.098	2.100	0.1	2.098	2.100	0.1	0.000	0.000	0.000
2	2.519	2.546	1.1	2.759	2.811	1.9	0.100	0.109	0.009
3	2.779	2.755	−0.9	3.288	3.399	3.4	0.200	0.261	0.061
4	3.033	2.962	−2.3	3.431	3.521	2.6	0.140	0.206	0.066

Therefore, the inverted anisotropic coefficients should be regarded as effective values that could be distorted by vertical inhomogeneity above the receiver. Still, our results are indicative of nonnegligible anisotropy in the predominantly carbonate section above the reservoir at Vacuum field.

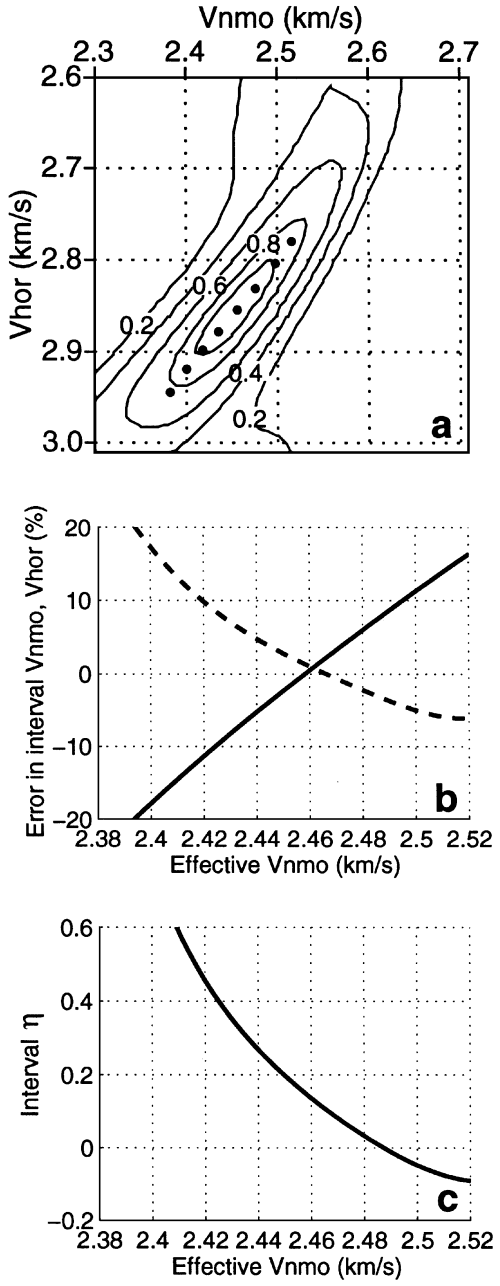

FIG. 8. (a) Semblance contours for the reflection from the bottom of the model (interface 4) described in Table 1. The semblance analysis was carried out using equation (10) on ray-traced synthetic data (Figure 7) for the spreadlength-to-depth ratio of two. (b) Percentage errors in the interval V_{nmo} (solid) and V_{hor} (dashed) in the fourth layer. The interval velocities were calculated from the effective values picked along the ridge in the semblance contours marked by dots (the horizontal axis shows the effective NMO velocity). (c) The interval η found from V_{nmo} and V_{hor} (the actual interval $\eta = 0.14$).

DISCUSSION AND CONCLUSIONS

Long-spread P-wave moveout from horizontal reflectors in VTI media depends on the vertical traveltime, NMO velocity V_{nmo}, and the "anellipticity" parameter η; the latter can be replaced by the horizontal velocity V_{hor}. While V_{nmo} controls hyperbolic moveout on conventional-length spreads, η or V_{hor} is responsible for the nonhyperbolic portion of the moveout curve at offsets that exceed the reflector depth. The importance of obtaining η or V_{hor} from surface data cannot be overestimated because either of these parameters (in combination with V_{nmo}) is sufficient to perform all time-processing steps for P-waves in VTI media, including NMO correction, dip-moveout (DMO) removal, and time migration (Alkhalifah and Tsvankin, 1995). Also, η represents a potentially powerful lithology indicator that can be used, for instance, to discriminate between shales and sands (Alkhalifah et al., 1996).

Here, we have studied the possibility of recovering η and V_{hor} using the nonhyperbolic moveout equation suggested by Tsvankin and Thomsen (1994) and later rewritten in terms of V_{nmo} and η by Alkhalifah and Tsvankin (1995). We recast this equation as a function of V_{nmo} and V_{hor} and improved its accuracy on intermediate spreads by introducing an additional coefficient in the denominator. Without this correction, the best-fit parameters V_{nmo}, V_{hor}, and η, obtained from nonhyperbolic moveout inversion, deviate from the actual values with increasing η (e.g., for a single layer with $\eta = 0.3$, the inverted value is 0.24).

The high accuracy of this approximation, however, does not guarantee reliable determination of all parameters from P-wave long-spread moveout, even in the simplest model of a single VTI layer. Our study reveals a family of kinematically equivalent VTI models that have close reflection traveltimes even on long-spread gathers. For spreadlength equal to two reflector depths, variations in V_{nmo} and V_{hor} within the family of equivalent models have a comparable magnitude but the opposite sign. As a result, the corresponding absolute change in the parameter η is at least as large as the sum of the relative changes in V_{nmo} and V_{hor}. In one of the examples, we reduced the value of η from 0.16 to 0.09 and increased the NMO velocity by 2.5% without changing the traveltimes by more than 3 ms at any offset up to two reflector depths.

To confirm this observation, we carried out actual inversion of P-wave reflection travetimes in a horizontal VTI layer by applying nonhyperbolic semblance analysis based on our modified moveout equation. For noise-free data, the maximum semblance corresponds to the correct values of the parameters, although the difference in semblance within the family of kinematically equivalent models is very small. Addition of random traveltime errors reduces the value of semblance but does not noticeably move the semblance maximum from the correct position. However, long-period traveltime errors do change the inversion results, even if the magnitude of these distortions is small. The corresponding errors in V_{nmo} and V_{hor} are very moderate (several percent) and comparable (for spreadlength-to-depth ratio of at least 2), but they have opposite signs. Hence, in agreement with the results of traveltime analysis, the absolute error in η typically is twice as large as the relative error in V_{hor}. For instance, a linear error function with the magnitude varying from 4 ms at zero offset to -4 ms at the end of the spread reduced the inverted value of $\eta = 0.16$ in half. Long-period errors of such a small magnitude can be caused by a

variety of reasons, including ambient noise, errors in the statics correction, or minor low- or high-velocity lenses.

Alkhalifah (1997) notes that semblance velocity analysis is less sensitive to errors in reflection traveltimes than are purely kinematic (e.g., least-squares) inversion algorithms. However, since semblance is calculated along moveout curves, it cannot overcome the intrinsic ambiguity of the kinematic inverse problem.

Nonhyperbolic moveout in vertically inhomogeneous VTI media is caused not only by anisotropy but also by the vertical variations in the elastic coefficients. The interval values of V_{hor} and η may be obtained by a Dix-type differentiation procedure that involves both quadratic and quartic moveout terms. In essence, the above conclusions about the accuracy in the estimation of V_{hor} and η remain valid for stratified media as well. The interval horizontal velocity for spreadlengths close to twice the reflector depth can be recovered with an accuracy comparable to that for NMO velocity (the error, of course, becomes higher in thin layers). The tradeoff between V_{nmo} and V_{hor}, however, is amplified by the layer-stripping process, causing large errors in the interval η values.

We have verified some of our conclusions by processing a walkaway VSP data set acquired at Vacuum field, New Mexico, by CSM's Reservoir Characterization Project. The traveltimes used in the moveout inversion were recorded by a single borehole receiver for a wide range of source-receiver offsets. The moveout parameters, obtained by least-squares fitting of our nonhyperbolic moveout equation to the observed traveltimes, yielded the value of η close to 0.2. However, due to the tradeoff between V_{nmo} and V_{hor} in the presence of a substantial scatter in the traveltime measurements, we estimate that η may lie within the interval $0.09 < \eta < 0.32$ (models within this interval produce rms time residuals different by no more than ± 1.5 ms). In any case, these results are indicative of nonnegligible anisotropy that should be taken into account in seismic processing and reservoir characterization in this area.

An important practical issue is whether it is possible to use the parameters obtained from nonhyperbolic moveout inversion for seismic processing. Since all kinematically equivalent models provide a good approximation for long-spread moveout (despite having substantially different values of η), they are suitable for poststack time migration. However, models

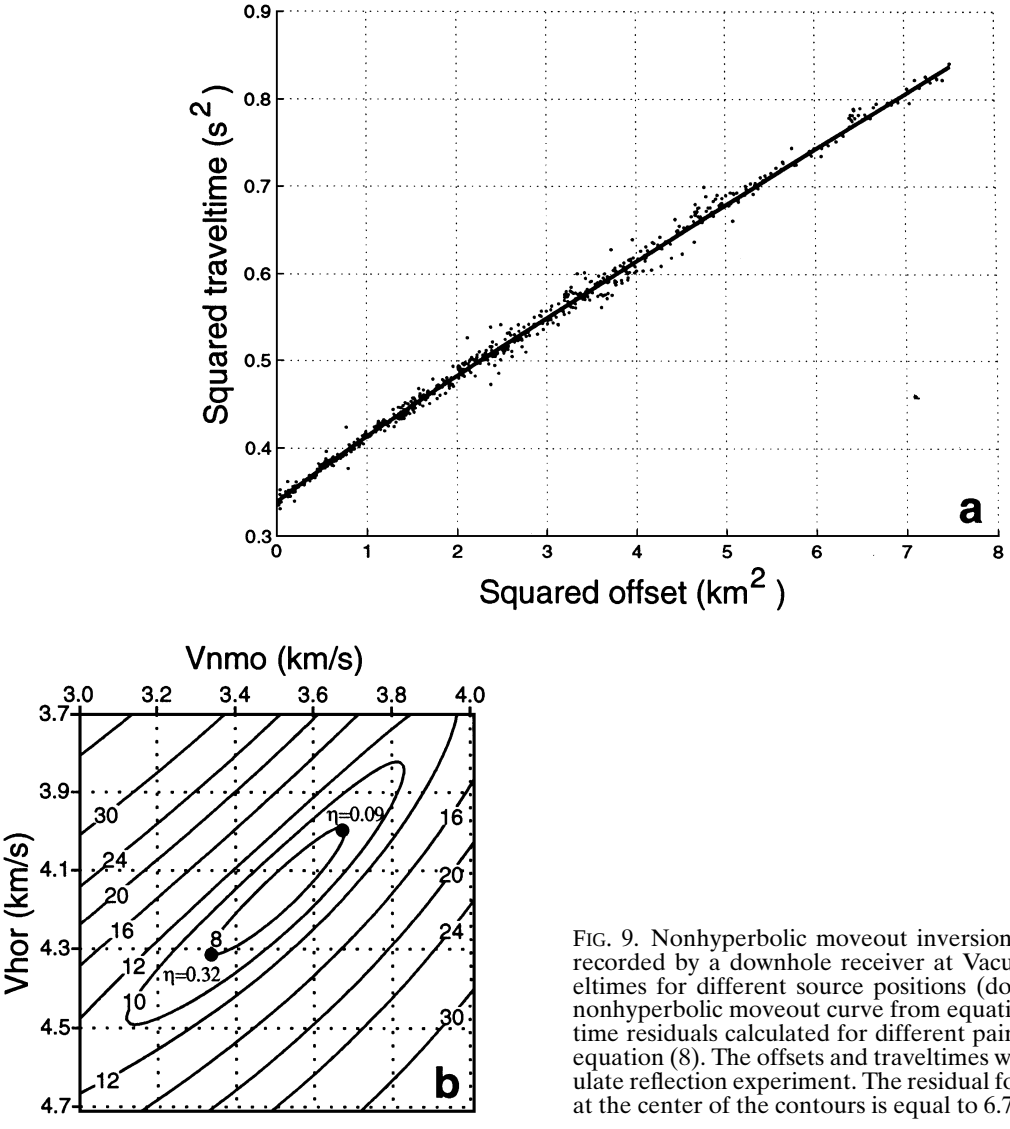

FIG. 9. Nonhyperbolic moveout inversion of the traveltimes recorded by a downhole receiver at Vacuum field. (a) Traveltimes for different source positions (dots) and the best-fit nonhyperbolic moveout curve from equation (8). (b) The rms time residuals calculated for different pairs (V_{nmo}, V_{hor}) using equation (8). The offsets and traveltimes were doubled to simulate reflection experiment. The residual for the best-fit model at the center of the contours is equal to 6.7 ms.

with the same nonhyperbolic moveout curves from horizontal reflectors do not necessarily yield the same DMO impulse responses, which may cause problems in anisotropic DMO processing.

Also, the need for imaging arises only in the presence of structure (i.e., dipping interfaces), and it is more natural to use imaging targets themselves for anisotropic parameter estimation. A more stable inversion method designed to obtain η from P-wave NMO velocity for dipping reflectors was developed by Alkhalifah and Tsvankin (1995). That approach, however, may experience difficulties in using steep events (e.g., from flanks of salt domes) with their small magnitude of reflection moveout. Since the horizontal velocity, primarily needed to image such steep dips, is much better constrained than is η by long-spread moveout, the results of nonhyperbolic moveout inversion in this case may be used to build a starting model for anisotropic migration. Another alternative, suggested by Grechka and Tsvankin (1996), is to obtain the horizontal velocity (or η) from the NMO velocity on a line parallel to the strike of a steep reflector.

Nonhyperbolic moveout inversion may be more difficult to use in lithology discrimination. In the absence of pronounced vertical inhomogeneity, the value of η obtained from nonhyperbolic moveout can be considered as a crude measure of anisotropy above the reflector, and, therefore, as a lithology indicator. However, the potentially large errors in interval η values may complicate a more detailed lithology analysis based on nonhyperbolic moveout inversion. Unfortunately, the horizontal velocity is much less suitable for lithology discrimination than η.

A more practical application of nonhyperbolic moveout inversion is estimation of Thomsen's parameter ϵ from reflection data in the case when the vertical velocity is known (e.g., from check shots or well logs). Errors in the coefficient η stem from the interplay between the horizontal and NMO velocity, while the vertical velocity is obtained independently. Therefore, it can be combined with the horizontal velocity recovered from long-spread moveout to provide an estimate of ϵ that will not be influenced by the error in $V_{\rm nmo}$.

ACKNOWLEDGMENTS

We are grateful to members of the A(nisotropy)-Team (especially Tariq Alkhalifah and Ken Larner) of the Center for Wave Phenomena, Colorado School of Mines, and Michel Le Bougeant of Imperial College, London, for useful discussions. Reviews by Ken Larner and an anonymous reviewer of *Geophysics* helped to improve the manuscript. We thank Bruce Mattocks and Bryan DeVault of the Reservoir Characterization Project at CSM for sharing the field data and helping in data processing. The support for this work was provided by the members of the Consortium Project on Seismic Inverse Methods for Complex Structures at CWP, Colorado School of Mines, and by the U.S. Dept. of Energy (project "Velocity Analysis, Parameter Estimation, and Constraints on Lithology for Transversely Isotropic Sediments" within the framework of the Advanced Computational Technology Initiative).

REFERENCES

Alkhalifah, T., 1997, Velocity analysis using nonhyperbolic moveout in transversely isotropic media: Geophysics, **62**, 1839–1854.

Alkhalifah, T., and Tsvankin, I., 1995, Velocity analysis in transversely isotropic media: Geophysics, **54**, 1550–1566.

Alkhalifah, T., Tsvankin, I., Larner, K., and Toldi, J., 1996, Velocity analysis and imaging in transversely isotropic media: Methodology and a case study: The Leading Edge, **15**, No. 5, 371–378.

Dix, C. H., 1955, Seismic velocities from surface measurements: Geophysics, **20**, 68–86.

Grechka, V., and Tsvankin, I., 1996, 3-D description of normal moveout in anisotropic media: 66th Ann. Internat. Mtg., Soc. Expl. Geophys., Expanded Abstracts, 1487–1490.

Hake, H., Helbig, K., and Mesdag, C. S., 1984, Three-term Taylor series for $t^2 - x^2$ curves over layered transversely isotropic ground: Geophys. Prosp., **32**, 828–850.

Neidell, N. S., and Taner, M. T., 1971, Semblance and other coherency measures for multichannel data: Geophysics, **54**, 1550–1566.

Taner, M. T., and Koehler, F., 1969, Velocity spectra—digital computer derivation and applications of velocity functions: Geophysics, **34**, 859–881.

Thomsen, L., 1986, Weak elastic anisotropy: Geophysics, **51**, 1954–1966.

Tsvankin, I., 1996, P-wave signatures and notation for transversely isotropic media: An overview: Geophysics, **61**, 467–483.

Tsvankin, I., and Thomsen, L., 1994, Nonhyperbolic reflection moveout in anisotropic media: Geophysics, **59**, 1290–1304.

———1995, Inversion of reflection traveltimes for transverse isotropy: Geophysics, **60**, 1095–1107.

APPENDIX A

DIX-TYPE INVERSION OF NONHYPERBOLIC MOVEOUT IN LAYERED MEDIA

P-wave reflection traveltime in vertically inhomogeneous VTI media is well-approximated by the following equation (Tsvankin and Thomsen, 1994):

$$t^2(x,i) = t_0^2(i) + A_2(i)x^2 + \frac{A_4(i)x^4}{1 + A(i)x^2}, \qquad \text{(A-1)}$$

where t_0 is the vertical traveltime and x is the source-receiver offset.

The quadratic moveout coefficient $A_2(i)$ is reciprocal to the squared NMO velocity

$$A_2(i) = \frac{1}{V_{\rm nmo}^2(i)}, \qquad \text{(A-2)}$$

while the parameter $A(i)$ is related to $A_2(i)$, the quartic moveout coefficient $A_4(i)$, and the horizontal velocity $V_{\rm hor}(i)$:

$$A(i) = \frac{A_4(i)}{V_{\rm hor}^{-2}(i) - A_2(i)}. \qquad \text{(A-3)}$$

Equations (A1)–(A3) are identical in form to the corresponding expressions for a homogeneous VTI medium; the parameters $A_2(i)$, $A_4(i)$, and $A(i)$, however, should be calculated for the stack of layers above the ith interface. NMO velocity $V_{\rm nmo}(i)$ in a layered VTI medium is given by the conventional Dix (1955) equation, while $A_4(i)$ can be obtained from an exact averaging formula that takes into account both anisotropy and vertical inhomogeneity (Hake et al., 1984). It is convenient to express $A_4(i)$ through η and NMO velocity in the same way as

in a single VTI layer (Alkhalifah, 1997):

$$A_4(i) = -\frac{2\eta(i)}{t_0^2(i)V_{\rm nmo}^4(i)}, \tag{A-4}$$

where $\eta(i)$ now represents an effective parameter that absorbs the influence of anisotropy and layering. An explicit expression for $\eta(i)$ can be obtained from the equation for $A_4(i)$ given in Hake et al. (1984) and Tsvankin and Thomsen (1994) (assuming $V_{S0,i} = 0$):

$$\eta(i) = \frac{1}{8}\left\{\frac{1}{V_{\rm nmo}^4(i)\,t_0(i)}\left[\sum_{i=1}^{N} V_{{\rm nmo},i}^4\,(1+8\eta_i)\,t_{0,i}\right] - 1\right\}, \tag{A-5}$$

where $V_{{\rm nmo},i}$, η_i, and $t_{0,i}$ are the interval values in layer i.

Since the meaning of the horizontal velocity in stratified media is not strictly defined, we assume (following Alkhalifah, 1997) that we can simply use equation (5), valid for homogeneous media:

$$V_{\rm hor}(i) = V_{\rm nmo}(i)\sqrt{1+2\eta(i)}\,, \tag{A-6}$$

where $V_{\rm nmo}(i)$ and $\eta(i)$ are the effective quantities defined above. Hence, $A_4(i)$ and $A(i)$ are now related to $V_{\rm nmo}(i)$ and $\eta(i)$ by the same expressions as in a single VTI layer, and equation (A-1) takes the form of equation (6):

$$t^2(x,i) = t_0^2(i) + \frac{x^2}{V_{\rm nmo}^2(i)} - \frac{2\eta(i)\,x^4}{V_{\rm nmo}^2(i)\left\{t_0^2(i)\,V_{\rm nmo}^2(i) + [1+2\eta(i)]\,x^2\right\}}. \tag{A-7}$$

Rewriting this expression in terms of the effective horizontal velocity, we obtain an analog of the single-layer equation (7),

$$t^2(x,i) = t_0^2(i) + \frac{x^2}{V_{\rm nmo}^2(i)} - \frac{\left[V_{\rm hor}^2(i) - V_{\rm nmo}^2(i)\right]x^4}{V_{\rm nmo}^2(i)\left[t_0^2(i)\,V_{\rm nmo}^4(i) + V_{\rm hor}^2(i)\,x^2\right]}. \tag{A-8}$$

In the main text, we introduce the coefficient C in front of the term $V_{\rm hor}^2 x^2$ and discuss the accuracy of this moveout approximation.

The moveout coefficients in equation (A-8) can be obtained from semblance analysis and used in a layer-stripping procedure. The interval NMO velocity can be recovered from the effective $V_{\rm nmo}(i)$ by the conventional Dix differentiation. To determine the interval values of the horizontal velocity and the parameter η, we use the Dix-type formulation of Tsvankin and Thomsen (1994) based on the quantity f defined as

$$f(i) \equiv V_{\rm nmo}^4(i)\left[1 - 4A_4(i)t_0^2(i)V_{\rm nmo}^4(i)\right].$$

In our notation,

$$\begin{aligned} f(i) &= V_{\rm nmo}^4(i)\left[1+8\eta(i)\right] \\ &= V_{\rm nmo}^2(i)\left[4V_{\rm hor}^2(i) - 3V_{\rm nmo}^2(i)\right]. \end{aligned} \tag{A-9}$$

From equations (A-5) and (A-9) it follows that

$$\begin{aligned} f(i) &= \frac{1}{t_0(i)}\sum_{i=1}^{N} V_{{\rm nmo},i}^4\,(1+8\eta_i)\,t_{0,i} \\ &= \frac{1}{t_0(i)}\sum_{i=1}^{N} V_{{\rm nmo},i}^2\left[4V_{{\rm hor},i}^2 - 3V_{{\rm nmo},i}^2\right]t_{0,i}. \end{aligned} \tag{A-10}$$

Hence, Dix-type differentiation of equation (A-10) allows us to find the interval values η_i and $V_{{\rm hor},i}$:

$$V_{{\rm hor},i} = V_{{\rm nmo},i} \times \sqrt{\frac{1}{4V_{{\rm nmo},i}^4}\,\frac{f(i)\,t_0(i) - f(i-1)\,t_0(i-1)}{t_0(i) - t_0(i-1)} + \frac{3}{4}} \tag{A-11}$$

and

$$\eta_i = \frac{1}{8V_{{\rm nmo},i}^4}\left[\frac{f(i)t_0(i) - f(i-1)t_0(i-1)}{t_0(i) - t_0(i-1)} - V_{{\rm nmo},i}^4\right]. \tag{A-12}$$